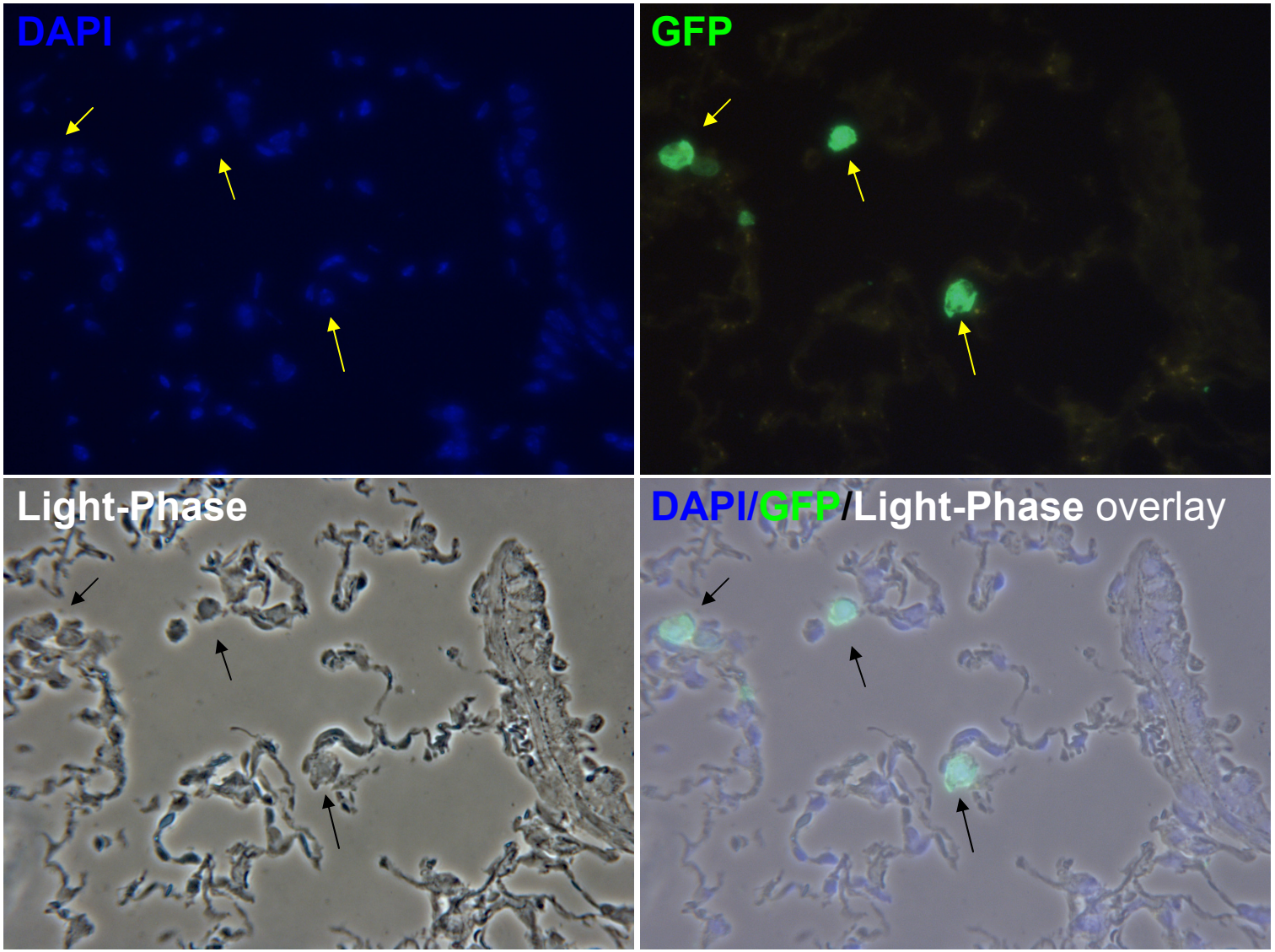

<u>Supplementary Figure 1</u>: Fluorescence microscopy of lung frozen tissue sections 2 months after intratracheal instillation of CMV-GFP lentiviral vector. Nuclei stained blue with DAPI; GFP=green fluorescence; phase-contrast microscopy overlay is used to show lung parenchymal histology. Note GFP+ cells (arrows) have typical morphology and intra-alveolar location of resident alveolar macrophages.

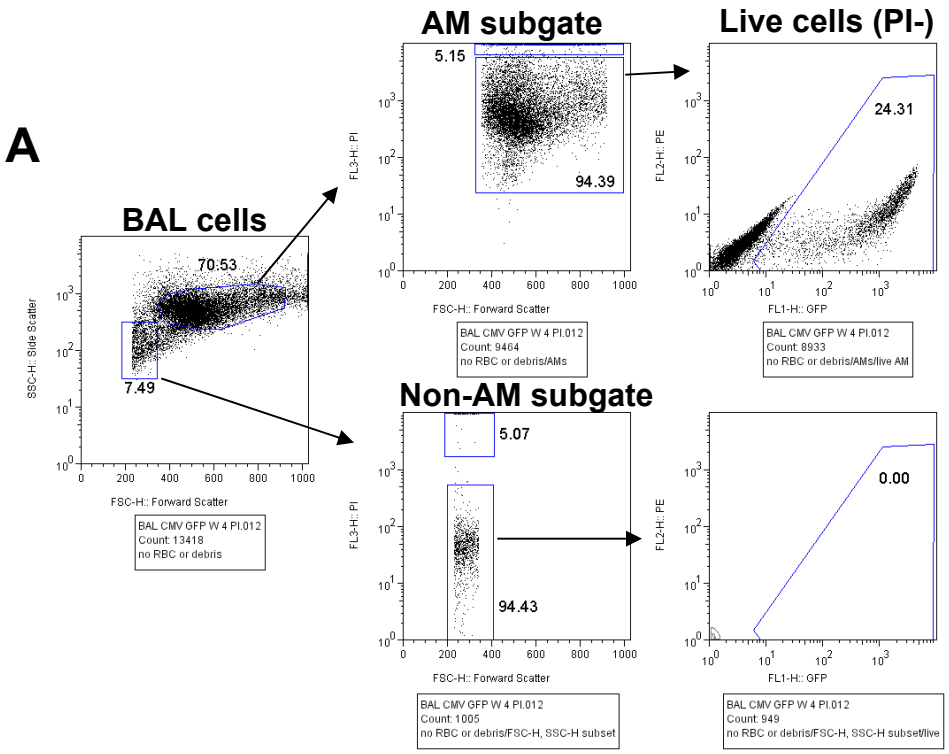

<u>Supplementary Figure 2</u>: Flow cytometry analysis of alveolar macrophages (AMs) obtained by BAL after lentiviral transduction with GFP-expressing lentiviral vectors. (A) Illustration of gating algorithm used to analyze live AMs within a BAL population, 1 year after infection with CMV-GFP lentivirus. Side scatter high/forward scatter high gating identifies AMs. Side scatter low/forward scatter low identifies the few non-AM cells in a normal BAL population (predominantly monocytes and lymphocytes, with rare neutrophils). Note high autofluorescence (FL3H:PI channel) of AMs compared to non-AMs. The brightest propidium iodide stained cells are considered dead (5% in each population) and excluded from analysis. Note: only cells within the 'live AM subgate' are transduced with GFP (=24% transduction efficiency). No GFP+ cells are found in the live non-AM subgate.
(B) Analysis of GFP expression in BAL after subgating on only live AMs (using the algorithm shown in A). Samples from four individual mice 1 year after infection with CMV-GFP lentiviral vector are shown.

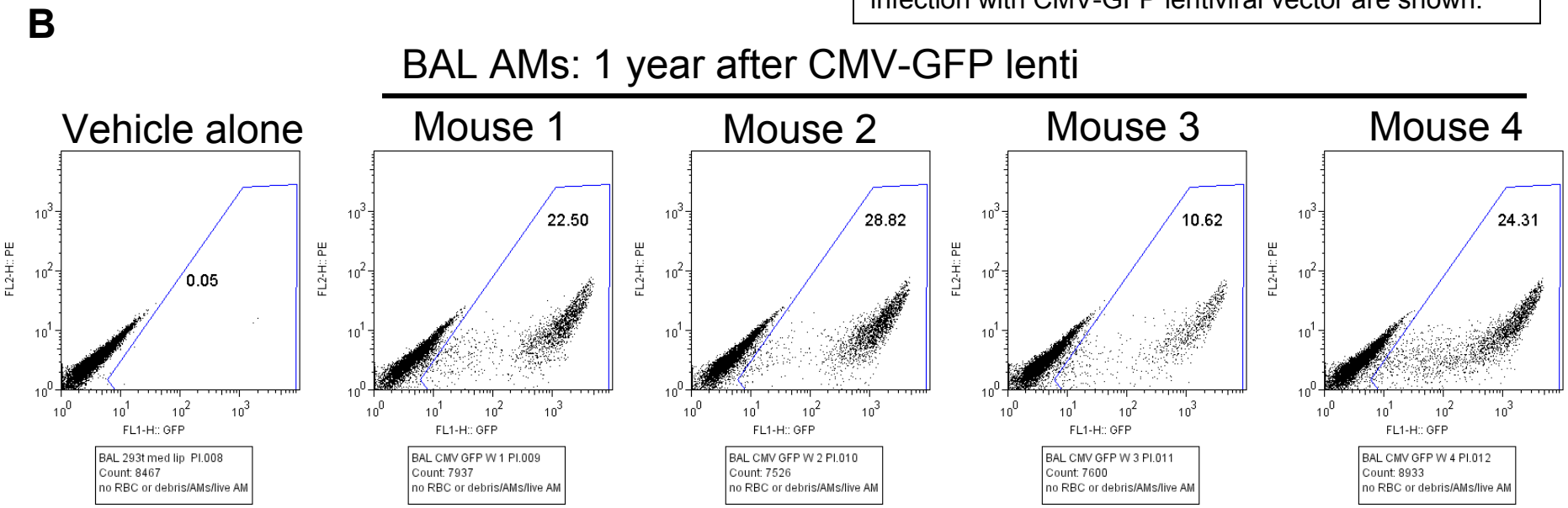

Supplementary Figure 3: MHC class II (1A/1E) cell surface expression levels on alveolar macrophages (AMs) quantified by flow cytometry 6 weeks after lentiviral infection. Unperturbed (uninfected) AMs exhibit dim MHC-II cell surface staining. In mice infected with 10^6 or 10^7 lentiviral particles, MHC-II levels (quantified by mean fluorescence intensity; MFI) are unchanged from baseline. In contrast, a representative mouse receiving 10^8 particles demonstrates more than 2 fold elevation in MFI in AMs, regardless of AM transduction status (GFP+, or GFP-). MFI values represent the average values from 10,000 AMs obtained by BAL from each mouse. Isotype control antibody shown to demonstrate specificity of MHC-II staining.

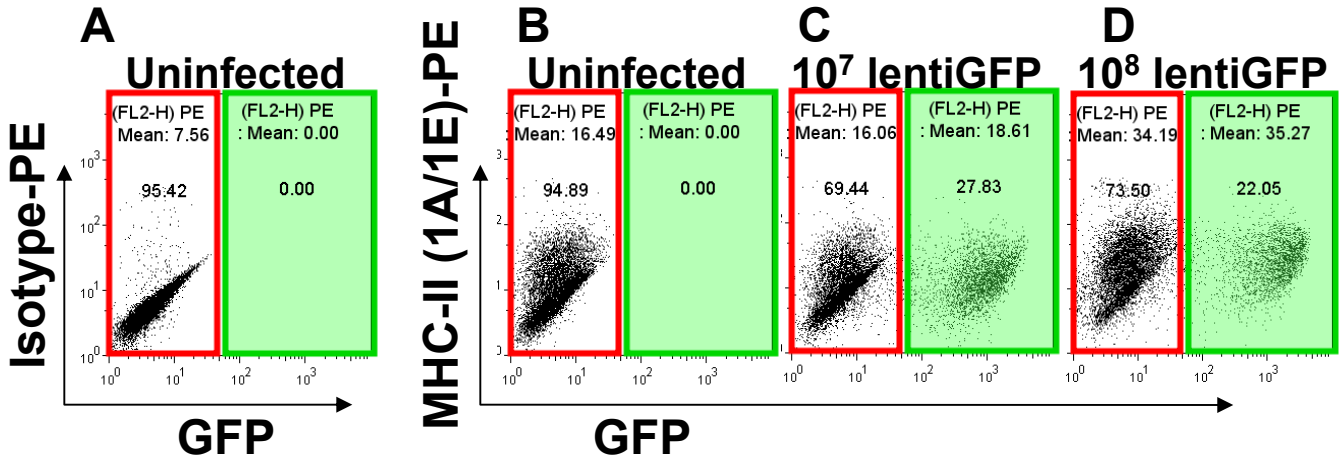

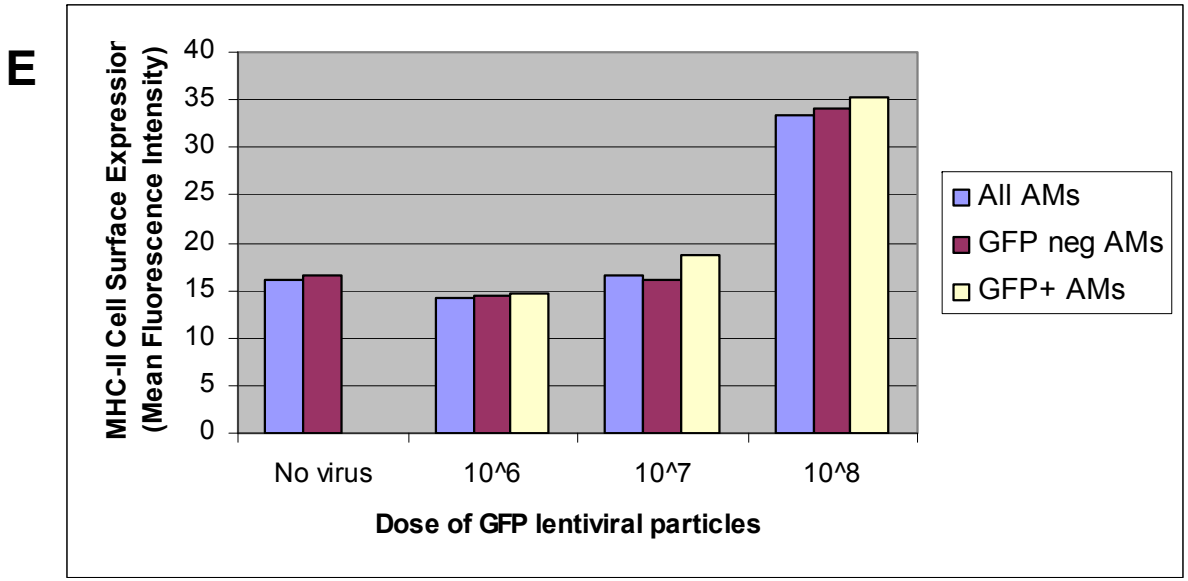

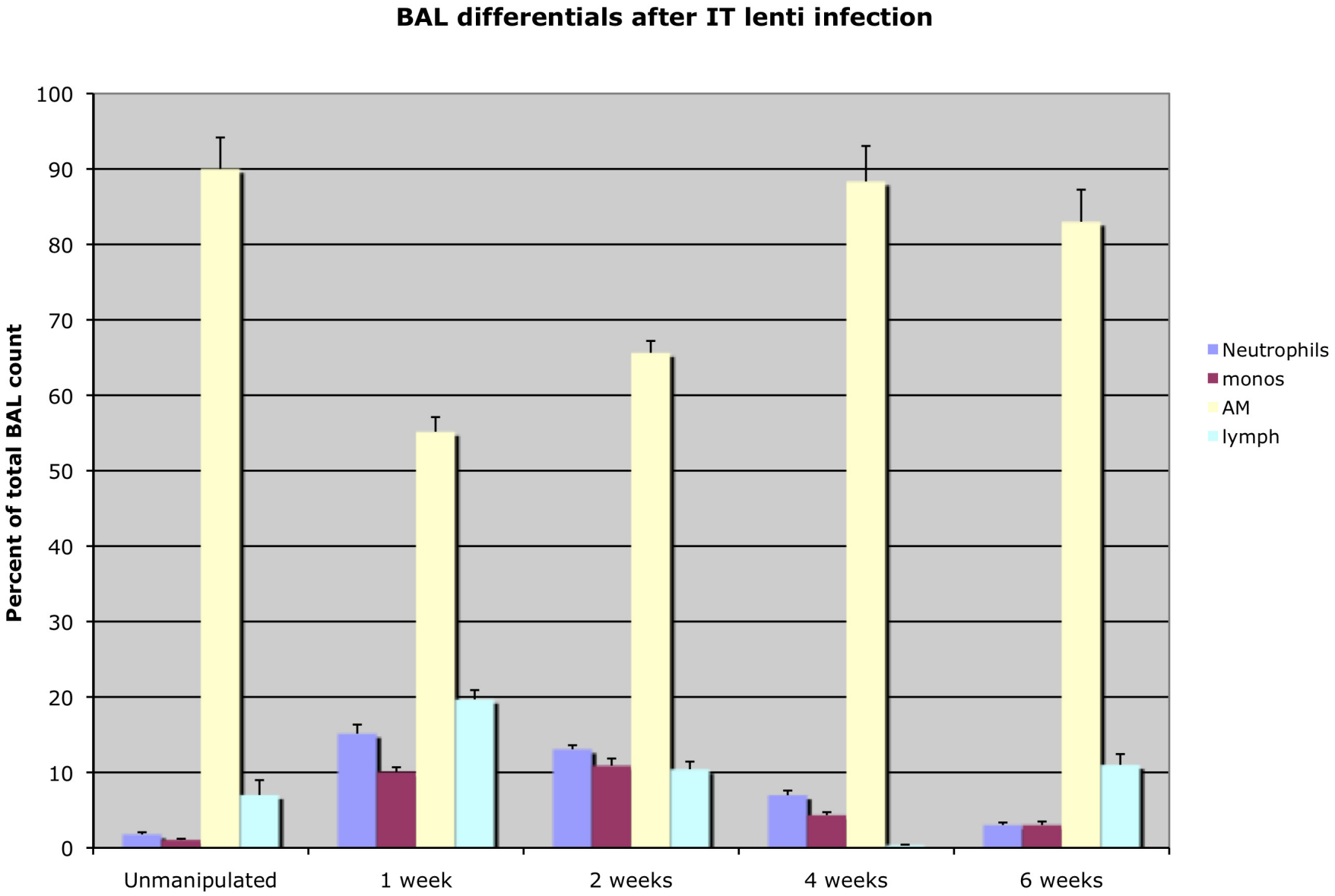

<u>Supplementary Figure 4</u>: Cytospin BAL differentials after IT lentiviral infection. Compared to unmanipulated mice, IT lenti-treated mice have transient increases in lavagable neutrophils, monocytes, and lymphocytes. This inflammation is maintained until 2 weeks after infection and completely resolves by 6 weeks, when the lavage characteristics are identical to those of an unmanipulated mouse.

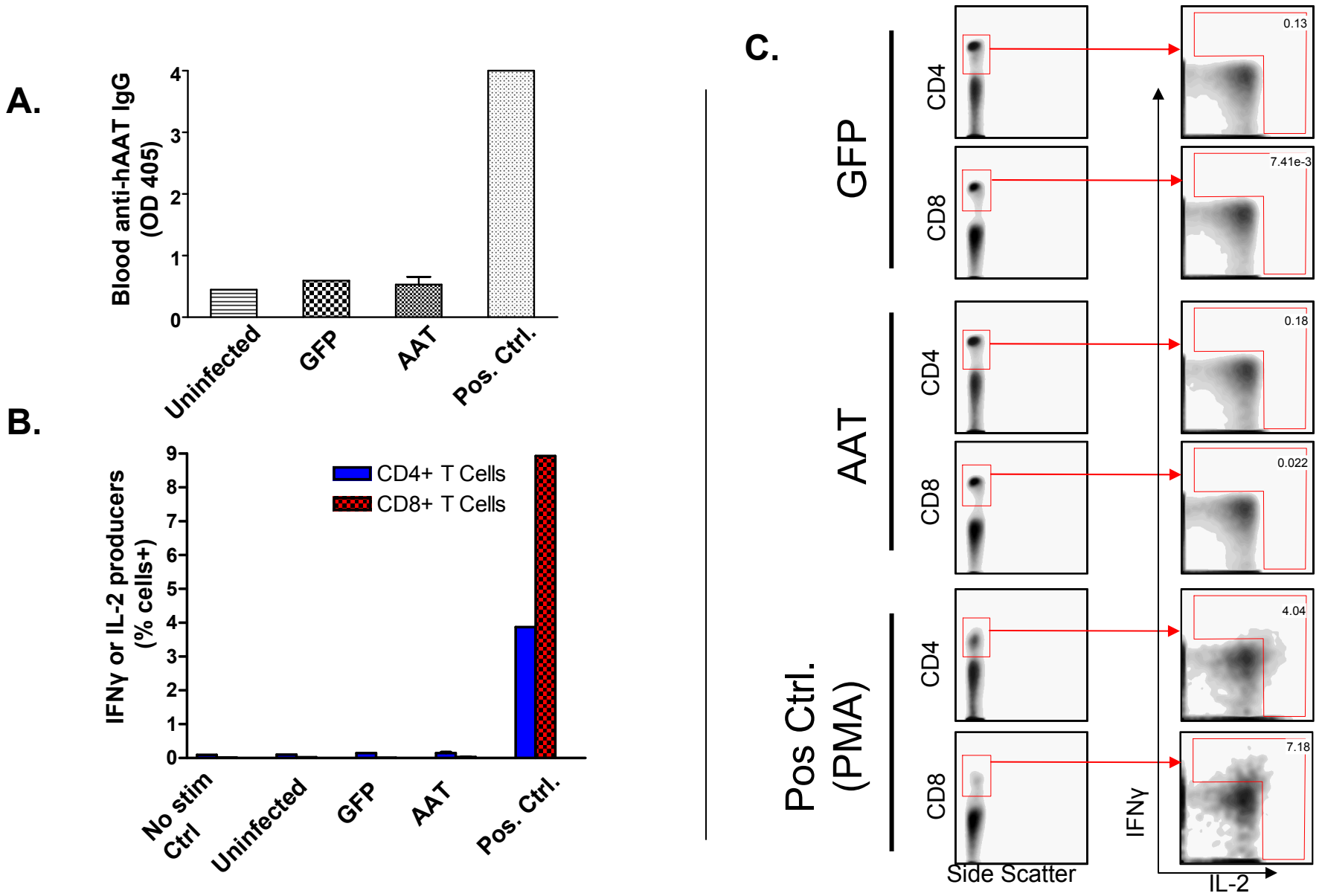

<u>Supplementary Figure 5</u>: Absence of cellular or humoral immune responses after expression of EF1α-hAAT lentiviral vector in vivo for 24 weeks. (A) ELISA results reveal no evidence of circulating IgG antibodies against hAAT detected in mice (n=4) treated with EF1α-hAAT lentivirus. (B) Summary graph of intracellular cytokine staining (ICS) of CD4+ and CD8+ T cells. Splenocytes were harvested from mice treated with EF1α-GFP ('GFP') or EF1α-hAAT ('AAT') lentiviruses (n=4 per group) and were stimulated (vs. no stimulation control) with hAAT protein. IFNγ and IL-2 production (indicating a T cell response to hAAT antigen) was quantified by FACS in each T cell subset. (C) Representative FACS plots from hAAT-stimulated splenocytes used to generate the graph in B are shown. Pos Ctrl=PMA+ionomycin stimulated splenocytes.

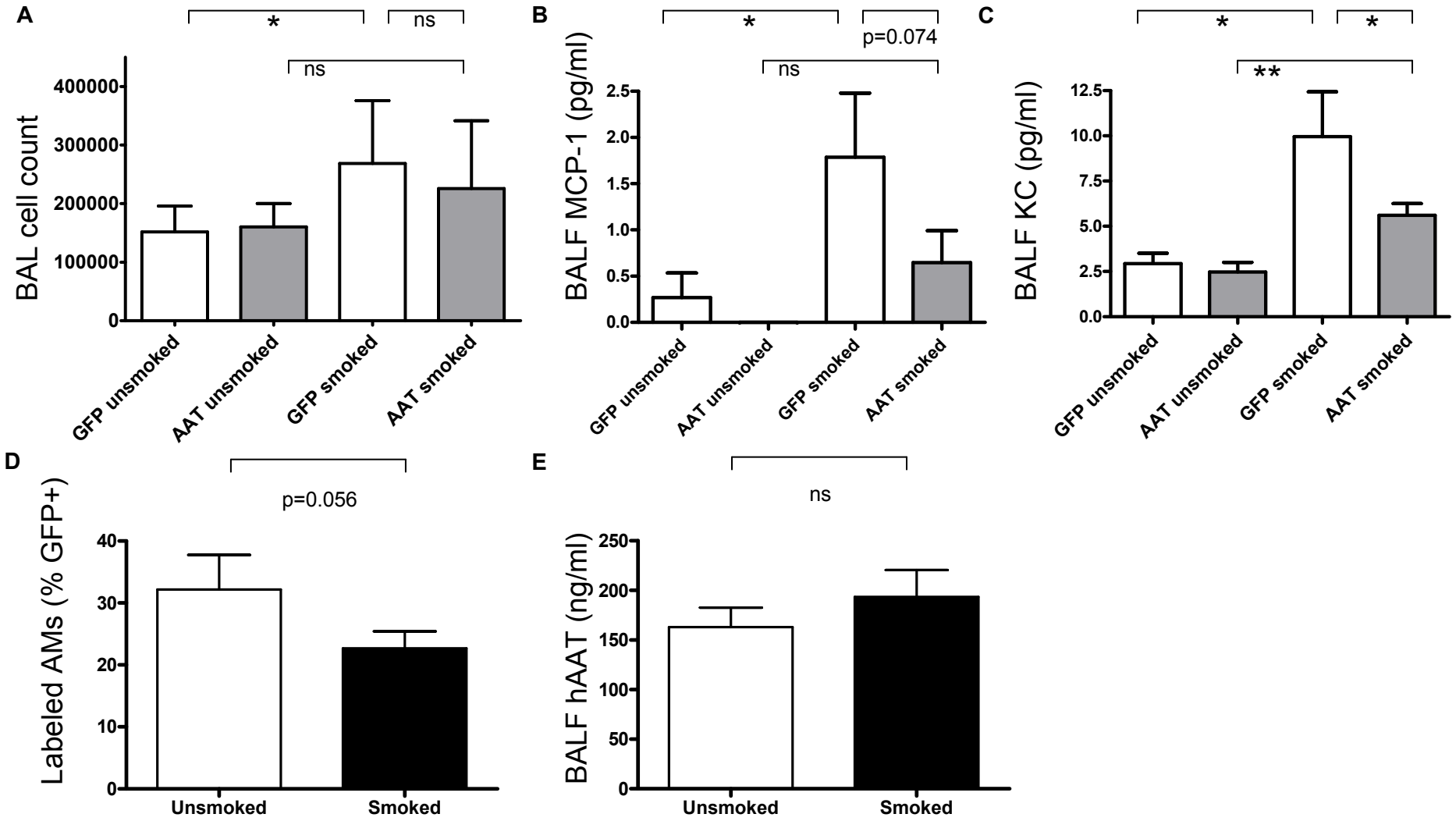

<u>Supplementary Figure 6</u>: Effects of lentiviral-based hAAT overexpression on acute cigarette smoke (CS) induced inflammation. (A) Ten days of CS exposure results in an increase in BAL cells in mice pre-treated with EF1a-GFP lentivirus (GFP), but not in mice pre-treated with EF1a-hAAT lentivirus (AAT) (n=10 per group); however, there is no statistically significant difference between GFP and AAT pre-treated groups. (B-C): Effects of acute CS exposure on select proinflammatory cytokines in the BALF. Ten days of CS exposure results in an increase in levels of MCP-1 and KC in BALF in mice pre-treated with GFP. AAT pre-treatment significantly ameliorates CS-induced KC elevation, but does not reach a statistically significant effect on MCP-1 elevation. (D-E) Persistence of lentiviral-based gene expression from transduced AMs in the setting of acute CS-induced inflammation. After 10 days of CS exposure, FACS-analysis of BALs (D) reveals persistence of lentivirally transduced AMs expressing the GFP reporter gene in mice pre-treated with EF1a-GFP lentivirus. Similarly, hAAT protein levels persist in the BALF of mice pre-treated with EF1a-hAAT (E). **=p<0.01; *=p<0.05 (Student¹s t-test).

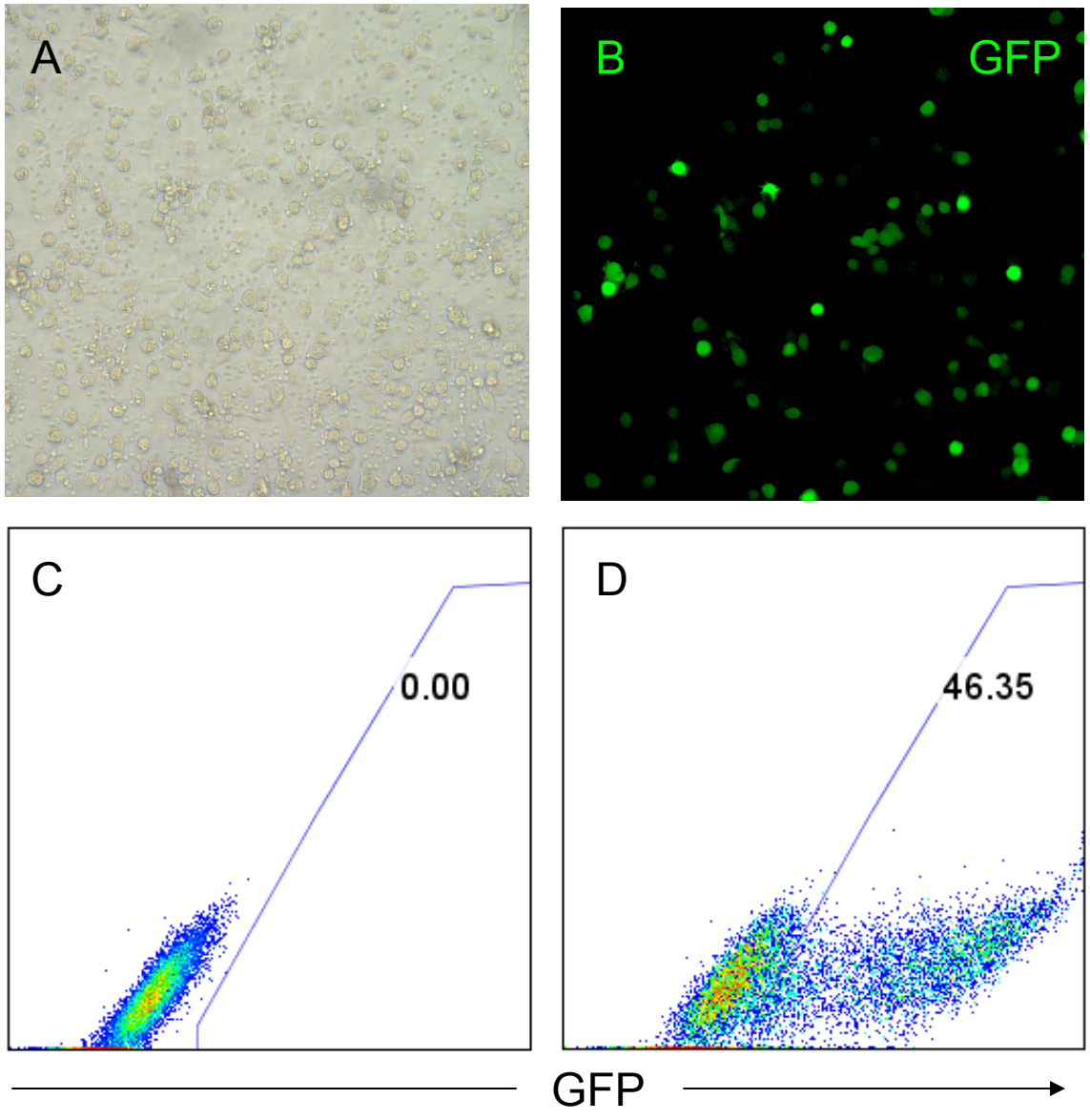

<u>Supplementary Figure 7</u>: Transduction of primary human alveolar macrophages. Human alveolar macrophages were isolated by bronchoalveolar lavage. After 24 hours in culture, they were infected overnight with lentivirus containing the GFP gene (CMV-GFP). 72 hours after infection, light (A) and fluorescence (B) microscopy images demonstrate GFP+ transduced cells. Flow cytometry indicates that approximately 46% of the AMs are GFP+ (D) as compared to the negative control (Mock infected) population (C).

Supplementary Methods

Vector packaging and design. cDNAs encoding the reporter genes (enhanced green fluorescence protein [GFP], firefly luciferase, and E.Coli lacZ) were ligated into the first gene position of the pHAGE lentiviral construct(1) by standard directional cloning into compatible NotI and BamHI sites. In order to track transduced cells by multiple methods within an individual animal, we modified the pHAGE vector for bicistronic dual transgenesis as follows: enhanced green fluorescence protein (GFP, Clontech) cDNA was amplified by PCR attaching NotI and Bam HI restriction sites to the 5' and 3' ends respectively. This amplicon was cloned into the pHAGE backbone in the first gene expression position by ligation to NotI/BamHI cohesive ends. Immediately upstream of the GFP ATG start site, the phosphoglycerate kinase (PGK, 464 bps) promoter was inserted. Next, cDNA encoding the luciferase gene from the firefly *Photinus pyralis* was generated by PCR attaching NdeI and ClaI sites to the 5' and 3' ends respectively for ligation into the second gene position of pHAGE. The internal ribosome entry site (IRES) from the encephalomyocarditis virus was inserted immediately upstream of the second cistron's ATG start site.

For hAAT gene expression, the cDNA encoding normal human alpha-1 antitrypsin (hAAT) was amplified by PCR from the C-AT plasmid(2), a generous gift of Drs Sihong Song and Terry Flotte (University of Florida, Gainseville). The hAAT cDNA was ligated into the first gene expression position of pHAGE as previously published(3), and the promoter elements indicated in the text (PGK, UBC, 0.2kb EF1a short, or 1.2kb EF1a long) were ligated immediately in front

of the hAAT ATG start site. VSV-G pseudotyped lentiviral particles were generated through transfection of 293T packaging cells with the pHAGE lentiviral backbone together with 4 helper plasmids encoding gag/pol, rev, tat, and VSV-G viral genes. Packaging and titering protocols along with plasmid maps and sequences are available for free download from www.kottonlab.com.

Alpha-1 antitrypsin measurement and analysis. hAAT protein expression in blood and BAL fuid specimens was measured by ELISA(3) (protocol generously provided by Drs. Roberto Calcedo and Joanita Figueredo, University of Pennsylvania, Philadelphia, PA). 96-well microtiter plates (Fisher Scientific, Pittsburgh, PA) were coated with rabbit anti-human alpha-1 antitrypsin antibody (Sigma #A 0409) as capture antibody followed by blocking with 3% bovine serum albumin (BSA; Sigma) in PBS. Standards were generated by serial dilutions of human alpha-1 antitrypsin (Sigma) in PBS with 0.5% BSA and 0.05% Tween 20 (Pierce Biotechnology, Rockford, IL). Samples and standards were plated in duplicate and incubated at 4ºC overnight followed by peroxidase conjugated goat anti-human AAT antibody (EY Laboratories, San Mateo, CA, #PA-2115-1). hAAT was quantified by optical densitometry after incubation with ABTS peroxidase substrate solution (Kirkegaard and Perry Laboratories, Gaithersburg, Maryland). The lower limit of detection for hAAT was 0.39 ng/ml. Measured urea values in the BAL fluid and blood (Quantichrom Urea Assay, Bioassay Systems, Hayward, CA) were used to calculate a dilution factor in order to quantify the original lung epithelial lining fluid (ELF) hAAT concentration for each animal(4). To understand hAAT ELF levels in the context of normal mouse endogenous AAT levels, these values were compared to estimated mouse epithelial lining fluid (ELF) AAT levels. Based on the known serum mouse AAT level of 2.85

mg/ml (5;6), the mouse ELF concentration of endogenous mouse AAT protein is approximately 340 mcg/ml (7)

Immune response. Serum and splenocytes were collected from recipient mice 24 weeks after treatment with intratracheal lentivirus. Cells were then washed with PBS + 2% FBS, counted, and resuspended (4×10^6 cells per tube) in RPMI 1640 medium (Cellgro, Herndon, VA.) supplemented with 10 % FBS, 25 mM HEPES, 2 mM l-glutamine, 20 U of penicillin per ml, 20 μg of streptomycin per ml, 1 mM sodium pyruvate and 0.1 mM nonessential amino acids. T cells from splenocyte samples were stimulated by incubation with anti-CD28 (2 μg/ml), anti-CD49d (2 μg/ml) and hAAT whole protein (4 μg/ml).

Unstimulated cells were incubated with the above reagents except for the protein. The cells were incubated at 37°C for 5 hr and Golgi Plug (BD Biosciences, 2 μl/ml) was added before an additional 12 hr incubation period. Positive control splenocytes were incubated for 6 hr with PMA (2 μg/ml) and Ionomycin (10 μg/ml) and Golgi Plug. After incubation, samples were washed with PBS + 2% FBS and stained with anti-CD8 and anti-CD4 antibodies for 15 min. Permeabilization was performed with Cytofix/Cytoperm solution (BD Biosciences). Cells were washed with 1× Perm/Wash buffer (BD Biosciences) and then stained with antibodies specific to IFN-γ and IL-2 for 30 min. After an additional washing step with 1× Perm/Wash buffer, cells were fixed in 2% formaldehyde-PBS. Cells were analyzed on an LSR II instrument (BD Bioscience) using FlowJo software (Treestar) to quantify the percentage of CD4+ and CD8+ lymphocytes producing IFN-γ and IL-2 in response to hAAT stimulation.

.

Splenocytes from individual mice were also stained with CFSE dye (1μM/ml) for 30 min at 37º C. The cells were then washed and plated in 96-well plates (4×10^6 cells/well). Cells were then stimulated in culture with or without hAAT protein (5μg / ml) for 96 hr at 37º C. The samples were then collected, stained with fluorescence-conjugated monoclonal antibodies against CD8, CD4 and CD19 (BD Bioscience), and run on the LSR II cytometer, followed by analysis with FlowJo software. Proliferation of CD4+ or CD8+ lymphocytes in response to hAAT stimulation was calculated by quantifying any dilution in CFSE staining for each cell population.

Sera were analyzed for the presence of circulating anti-hAAT-specific IgG antibodies by ELISA. Ninety-six-well plates (Maxisorp, Nunc) were coated overnight at 4°C with 1 μg of the recombinant hAAT antigen/well in 0.1M sodium carbonate (pH 9.5) solution. Plates were washed twice with PBS-0.05% Tween 20 and blocked with PBS-10% FCS (2 hr at room temperature). Subsequently, mouse serum samples diluted serially in PBS were added to the wells for 2 hr incubation at RT. Serial dilutions of hAAT specific rabbit polyclonal serum were added as positive controls. Plates were then washed 5 times with PBS-0.05% Tween 20, and either HRP-conjugated goat anti-mouse IgG (KPL) or HRP-conjugated goat anti rabbit IgG (BIORAD) as appropriate. After incubation for 1 h at room temperature, plates were washed 7 times and Sure Blue reagent (KPL) was added. Reactions were stopped after 30 min by addition of TMB stop solution (KPL). Absorption was read at 405 nm using an ELISA reader (SPECTRA max PLUS).

Lung physiology: impedance measurements. Mice were deeply anesthetized by intraperitoneal injection of pentobarbital sodium (70 mg/kg) and then tracheostomized and cannulated in the

supine position. The cannula was connected to a computer-controlled ventilator (Flexivent, SCIREQ, Montreal, Canada). Mice were mechanically ventilated with room air; a tidal volume of 8 ml/kg at a frequency of 240 breaths/min was used. Dynamic respiratory mechanics were measured at four different positive end-expiratory pressure (PEEP) levels (0, 3, 6, and 9 cmH2O) in the closed-chest condition and assessed by measuring impedance data during forced oscillations. To standardize volume history, each measurement was preceded by two consecutive inflations of the lungs to total lung capacity. Impedance data collection was made by interrupting mechanical ventilation for 6 s by use of the optimal ventilation waveform (OVW), which is a broadband waveform containing energy from 0.5 to 15 Hz(8). The frequencies in the OVW are selected according to a nonsum-nondifference criterion, which eliminates harmonic distortion and minimizes cross talk among the frequencies present in the input flow waveform and hence provides smooth estimates of the input impedance(9). The volumes delivered are similar to normal spontaneous tidal volume values; hence, the method provides information on the mechanical properties during conditions mimicking breathing. The peak-to-peak OVW amplitude was matched to the tidal volume delivered by the mechanical ventilator individually in each mouse. The ventilator displacement and cylinder pressure signals were low-pass filtered at 30 Hz and sampled at 256 Hz. With the use of Fourier analysis, impedance spectra were calculated on overlapping blocks of pressure, and flow data and were calculated as the ratio of the cross-power spectrum of pressure and flow to the autopower spectrum of flow. The forced oscillatory system was calibrated by measuring the input impedance of known analogs, including tubes and bottles with known impedances. The frequency response of the system was obtained, and the measured impedance spectra were off-line corrected for any phase difference between

pressure and flow. Additionally, the flow-dependent impedance of the tracheal cannula was characterized separately and removed from the respiratory impedance of the mice.

Lung physiology: impedance modeling. To interpret the impedance spectra, we used a 4-parameter model of the respiratory system, called the constant phase (CP) model(10), which is composed of a linear tissue impedance ($\underline{Z_{ti}}$) and airway impedance (Z_{aw}). The Z_{ti} is calculated as:

$$Z_{ti}(\omega_n) = (G - jH)/\omega_n^{\alpha}, \text{ with } \alpha = 2/\pi \arctan(H/G) \text{ and } \omega_n = \omega/\omega_0$$

where ω_n and ω are the normalized and absolute circular frequency, G and H are the coefficients of tissue damping and elastance, respectively, and j is the imaginary unit. The exponent α describes the frequency dependence of tissue resistance ($R_{ti} = G/(\omega_n)^{\alpha}$) and tissue elastance ($E_{ti} = H(\omega_n)^{1-\alpha}$). The normalization factor $\omega_0 = 1$ rad/s is used to obtain meaningful units for the parameters G and H. The respiratory system impedance is obtained by adding Z_{aw} in series to Z_{ti} where Z_{aw} is the series combination of R_{aw} and an airway inertance (I_{aw}).

$$Z_{aw}(\omega_n) = R_{aw} + j\omega I_{aw}$$

There are four parameters to estimate from the impedance spectra: R_{aw}, I_{aw}, G and H.

Tissue compliance (C) is calculated as the reciprocal of elastance: C=1/H

Quantification of lung emphysema by histology. First, the original histological image captured was thresholded to obtain a binary image, with black representing tissue and white representing airspace. The threshold level was computed automatically from the original image. To measure airspace area and diameter, the binary image was first segmented into distinct airspaces using the watershed transform as follows. From the binary image, first a distance map was calculated, such that every pixel representing air was replaced by the negative of the Euclidean distance between

that pixel and the nearest pixel representing tissue. The resulting distance map had basins corresponding to airspaces with separate regional minima. Every regional minimum with depth larger than a threshold value was identified with a unique label. Each labeled region was then grown by iteratively increasing the grayscale level. Pixels where two different labeled regions met were marked as boundary pixels which completed the segmentation process. The area of an airspace was then measured by counting the number of pixels inside a labeled region and scaling to physical dimensions. The corresponding equivalent airspace diameter was calculated as the diameter of a circle having the same area as the airspace. From the set of equivalent diameters, we computed the various moments and their ratios. Specifically, as shown by Parameswaran et al.(11), the index D_2, which is obtained as the third moment over the second moment of the equivalent diameter distribution, is an excellent index sensitive to small changes in airspace structure. It can be shown that D_2 is equal to the area weighted mean equivalent diameter and is a function of the mean, variance and skewness of the diameter distribution.

Supplementary Methods Reference List

1. **Murphy,G.J., Mostoslavsky,G., Kotton,D.N., and Mulligan,R.C. 2006. Exogenous control of mammalian gene expression via modulation of translational termination.** ***Nat. Med.*** **12:1093-1099.**

2. **Song S et al 1998. Sustained secretion of human alpha-1-antitrypsin from murine muscle transduced with adeno-associated virus vectors.** ***Proceedings of the National Academy of Sciences of the United States of America*** **95:14384-14388.**

3. **Wilson,A.A., Kwok,L.W., Hovav,A.H., Ohle,S.J., Little,F.F., Fine,A., and Kotton,D.N. 2008. Sustained Expression of {alpha}1-antitrypsin After Transplantation of Manipulated Hematopoietic Stem Cells.** ***Am. J. Respir. Cell Mol. Biol.***

4. **Rennard,S.I., Basset,G., Lecossier,D., O'Donnell,K.M., Pinkston,P., Martin,P.G., and Crystal,R.G. 1986. Estimation of volume of epithelial lining**

fluid recovered by lavage using urea as marker of dilution. ***J. Appl. Physiol*** **60:532-538.**

5. Takahara,H., Nakamura,Y., Yamamoto,K., and Sinohara,H. 1983. Comparative studies on the serum levels of alpha-1-antitrypsin and alpha-macroglobulin in several mammals. ***Tohoku J. Exp. Med.*** **139:265-270.**

6. Kushi,A., Akiyama,K., Noguchi,M., Edamura,K., Yoshida,T., and Sasai,H. 2004. Disruption of the murine alpha1-antitrypsin/PI2 gene. ***Exp. Anim*** **53:437-443.**

7. Wewers,M.D., Casolaro,M.A., Sellers,S.E., Swayze,S.C., McPhaul,K.M., Wittes,J.T., and Crystal,R.G. 1987. Replacement therapy for alpha 1-antitrypsin deficiency associated with emphysema. ***N. Engl. J. Med.*** **316:1055-1062.**

8. Lutchen,K.R., Yang,K., Kaczka,D.W., and Suki,B. 1993. Optimal ventilation waveforms for estimating low-frequency respiratory impedance. ***J. Appl. Physiol*** **75:478-488.**

9. Suki,B., and Lutchen,K.R. 1992. Pseudorandom signals to estimate apparent transfer and coherence functions of nonlinear systems: applications to respiratory mechanics. ***IEEE Trans. Biomed. Eng*** **39:1142-1151.**

10. Hantos,Z., Daroczy,B., Suki,B., Nagy,S., and Fredberg,J.J. 1992. Input impedance and peripheral inhomogeneity of dog lungs. ***J. Appl. Physiol*** **72:168-178.**

11. Parameswaran,H., Majumdar,A., Ito,S., Alencar,A.M., and Suki,B. 2006. Quantitative characterization of airspace enlargement in emphysema. ***J. Appl. Physiol*** **100:186-193.**